Original Research

ResolvinD1 attenuates high-mobility group box 1-induced epithelial-to-mesenchymal transition in nasopharyngeal carcinoma cells

Pingli Yang[1,3], Shan Chen[1], Gang Zhong[1], Yan Wang[1], Weijia Kong[1,2] and Yanjun Wang[1,2]

[1]Department of Otorhinolaryngology, Union Hospital, Tongji Medical College, Huazhong University of Science and Technology, Wuhan 430022, China; [2]Institute of Otorhinolaryngology, Union Hospital, Tongji Medical College, Huazhong University of Science and Technology, Wuhan 430022, China; [3]Department of Otorhinolaryngology, The First Affiliated Hospital, Shihezi University School of Medicine, Shihezi, Xinjiang 832000, China

Co-corresponding authors: Wei-Jia Kong, Email: entwjkong@hust.edu.cn; Yan-Jun Wang, Email: yanjunwangent@163.com

Impact statement

Nasopharyngeal carcinoma has a high incidence in China. Discussing the molecular mechanism of nasopharyngeal carcinoma is important because of high recurrent rate and low quality of life after treatment. HMGB1, as an important inflammatory factor, promotes the process in many cancers. But little is known about how HMGB1 affects the progress of nasopharyngeal carcinoma cells. In our research, we assessed the role of HMGB1 on metastasis and invasion of nasopharyngeal carcinoma cells. The result of study indicates HMGB1-induced EMT in nasopharyngeal carcinoma cells. Furthermore, we observed that RvD1, which plays an actively protective role in many diseases, controls the migration and invasion of nasopharyngeal carcinoma cells by inhibiting the HMGB1-induced EMT. RvD1 can be further studied as a protective factor for nasopharyngeal carcinoma.

Abstract

Epithelial-to-mesenchymal transition (EMT) process is prevalent during the progression of tumors. Nasopharyngeal carcinoma (NPC) is no exception. High-mobility group box 1 (HMGB1) was reported to have the effect of inducing EMT in malignancy. However, the impact of HMGB1-induced EMT in NPC is unclear. Resolvin D1 (RvD1) was reported to regress the progression of inflammation and apoptosis of phagocytes. The effect of RvD1 in the EMT is largely unknown. The current research explored the role of RvD1 on HMGB1-induced EMT in NPC. EMT markers were investigated in 10 NPC and 10 nasopharyngitis (NPG) patients using immunohistochemistry and Western blot. In vitro, expression of EMT markers and HMGB1 in CNE1 and CNE2 cells was assessed with immunohistochemical, Western blot, and confocal microscopy after treatment with recombinant human HMGB1 (rhHMGB1) or HMGB1 gene silencing or RvD1. The invasion and migration of NPC cells were detected by scratch test and transwell assay. Overexpression and gene silencing of lipoxin A4 receptor/formyl peptide receptor 2 (ALX/FPR2) and G protein-coupled receptor 32 (GPR32) in CNE2 cells confirmed the effect of RvD1 using Western blots. N-cadherin, vimentin, and HMGB1 were found up-regulated in NPC samples compared with NPG samples, while ZO-1 and E-cadherin were down-regulated in NPC tissues. RhHMGB1-induced EMT in CNE1 and CNE2 cells in a dose-dependent way. CNE2 cell lines treated with rhHMGB1 possessed greater invasion and migration ability, which was confirmed by gene silencing. RvD1 suppressed HMGB1-induced EMT in NPC cells via ALX/FPR2 and GPR32 receptors. These results showed that EMT was obvious in NPC. HMGB1 played a key role in inducing EMT. RvD1 inhibited HMGB1-induced EMT and might have potential application in the area of NPC treatment.

Keywords: Nasopharyngeal carcinoma, high-mobility group box 1, epithelial-to-mesenchymal transition, Resolvin D1

Experimental Biology and Medicine **2019; 244: 1608–1618. DOI: 10.1177/1535370219885320**

Introduction

Nasopharyngeal carcinoma (NPC) arises from the epithelium of the nasopharynx. The highest rates of NPC are in southeast Asia and northern Africa.[1] The onset of NPC in the population gradually increases from the age of 20 to 60. Genes, viruses, and environment have been implicated in the occurrence of NPC. Histologically, NPC is divided into squamous-cell carcinomas and non-keratinizing carcinomas, with most cases being non-keratinizing (>95%).[2] Further understanding the mechanism of NPC recurrence

and metastasis will help us to improve therapeutic efficacy and clinical outcomes.

The transition of epithelial and endothelial cells to a motile phenotype, i.e. epithelial-to-mesenchymal transition (EMT), has been demonstrated to be related to several biological and pathological processes such as embryonic development, inflammation, and carcinoma. The cell morphology changes from the epithelial cell phenotype into a spindle fibroblast-like appearance during EMT, which gives mobile features to cells. Thus, EMT induces the acquisition and enhancement of invasive ability in cancer cells. The core events in EMT are the loss of the cell connectivity and apical–basal polarity.[3] EMT has been shown to be related to cancer metastasis and poor prognosis in multiple cancers,[4–7] including NPC.[8] The EMT process is induced by a variety type of factors, such as IGF-II, EGF, FGF, TGF-β and Smad4, the microenvironment and matrix-degrading enzymes, such as MMPS, and miRNA. Recently, high-mobility group box 1 (HMGB1) was reported to enhance EMT in numerous cancers.

HMGB1 was associated with DNA synthesis, repair, transcription, and genomic stability. It also takes part in inflammation, chemotaxis, and tissue regeneration after active or passive protein release from the nucleus.[9] Different expression patterns of HMGB1 have been observed in numerous tumors, including lung, colorectal, cervical, and pancreatic cancers.[10–14] Increased expression of HMGB1 has been found in NPC and is associated with progression of the disease and a poor prognosis.[15,16] All these suggest that HMGB1 may promote NPC cell survival and invasion. As mentioned above, EMT plays a key role during cancer cell invasion and HMGB1 can enhance this process in various cell types. Thus, we hypothesize that HMGB1 may be implicated in the pathogenesis of NPC via promoting EMT.

Resolvin D1 (RvD1) is a pro-inflammatory extinction factor formed by DHA through enzymatic transformation in the inflammatory process, which can have an ultra-anti-inflammatory effect at the NK level.[17] RvD1 is a well-studied member of D series resolvin, which has protective effect in respiratory diseases and allergic diseases.[18] Previous studies found that RvD1 can alleviate the endothelial cell tight connection disorder and permeability change caused by lipopolysaccharide stimulation and effectively inhibit TGF-β1-induced EMT by binding to its receptors,[19,20] lipoxin A4 receptor/formyl peptide receptor 2 (ALX/FPR2), and G protein-coupled receptor 32 (GPR32), suggesting that RvD1 can effectively restore the epithelial barrier, reduce epithelial permeability, and reduce pathogen invasion. RvD1 has been reported as inhibiting tumor development by binding to its receptors. We speculated that RvD1 inhibits the proliferation and metastasis of NPC by inhibiting HMGB1-induced EMT.

Materials and methods

Cell lines and cell culture

Cells from the human nasopharyngeal carcinoma cell lines CNE1 (well differentiated) and CNE2 (poorly differentiated) were grown in Dulbecco's modified Eagle's medium (DMEM Hyclone, USA) containing 10% fetal bovine serum and 1% penicillin/streptomycin. The cells were incubated at 37°C in 5%CO_2. CNE1 and CNE2 were obtained from the cancer center of Union Hospital (Wuhan, China) in March 2018.

Patient tissue samples

Ten non-keratosis NPC tissue samples from patients diagnosed with NPC by histopathology examination, and 10 NPG tissue samples were obtained from the Department of Otolaryngology, Union Hospital (Wuhan, China) between December 2017 and October 2018. Some of the samples (two-thirds of the sample) were stored for biochemical detection, and some were fixed with formalin for morphological detection. The experiments were approved by the research ethics committee of Tongji Medical College, Huazhong University of Science and Technology (2018S440).

Protein extraction and Western blot

Tissue and cell protein expression levels were examined using Western blotting. The 10 NPC tissues and 10 NPG tissues and cells were dissected in radioimmunoprecipitation assay lysis solution (Beyotime, Haimen, Jiangsu, China) containing phosphatase inhibitors and PMSF. After detection of protein concentrations, approximately 20 μg of protein was loaded on 10% SDS polyacrylamide gels. Then, the extracted proteins were transferred from gel onto polyvinylidene fluoride (PVDF) membranes. The PVDF membranes were blocked with a blocking buffer (5% non-fat milk in tris-buffered saline and tween 20 (TBST)) for 1 h and then incubated overnight at 4°C with the following antibodies: ZO-1 (GTX108613,CA, USA, diluted 1:1000, rabbit polyclonal), N-cadherin (GTX127345,CA, USA, diluted 1:1000, rabbit polyclonal), E-cadherin (GTX100443,CA, USA, diluted 1:1000, rabbit polyclonal), vimentin (GTX112661, CA, USA, diluted 1:1000, rabbit polyclonal), HMGB1 (ab79823, diluted 1:10,000, Abcam, rabbit monoclonal). Membranes were washed three times with TBST and incubated 1 h with the horseradish peroxidase (HRP)-labeled secondary antibodies. Enhanced Chemiluminescent Plus (Beyotime, Haimen, Jiangsu, China) was used to visualize the membranes. The relative grayscale of the bands of protein and glyceraldehyde 3-phosphate dehydrogenase (GAPDH) were quantified using Image J 1.51J8 software.

Immunohistochemical staining

HMGB1 localization and transposition in the NPC and NPG tissues were analyzed. After fixed in 4% formaldehyde for at least 12 h, the tissue samples were dehydrated by graded ethanol, and soft and hard paraffin embedded. Finally, the tissues were cut into 5 μm sections and placed on glass slides.

The tissue sections went through de-paraffinization, hydration, heat-repair, and were blocked. Finally, the sections were incubated with HMGB1-antibody (Abcam,

diluted 1:350) at 4°C overnight. The second day, stained with diaminobenzidine (DAB) and hematoxylin, the slides were counted with a light microscope. The intensity of staining was scored with Image-Pro plus6.0.

Immunofluorescence

The protein expression of ZO-1 and vimentin in CNE2 cells was determined by immunofluorescence. After incubation with siHMGB1, recombinant human HMGB1 (rhHMGB1), or RvD1, cells were fixed with 4% paraformaldehyde and incubated with 0.1% Triton X-100 for 20 min to increase permeability. After washing with PBS three times, 3% BSA was used to saturate excess protein-binding sites, and primary antibody was incubated with cover slips overnight at 4°C. The second day, the primary antibody was removed. After washing three times with PBS, the cover slips were incubated with fluorescent antibody (Alexa Fluor 594 donkey anti-rabbit IgG) 1 h and stained with DAPI 5 min for the identification of nuclei at room temperature. After rinsing with PBS and sealing with antifade mounting medium, the cover slips were immediately placed on an Olympus immunofluorescence microscope (Nikon A1-si, Japan) for observation.

Wound-healing assay

The CNE2 cells were inoculated in six-well plates. After incubation overnight, the cells grew to over 90% confluency. A wound of cell monolayers was created using a sterile 200-μl plastic pipette tip. The cells were then treated with rhHMGB1 (500 ng/ml) or small interfering HMGB1 and cultured with serum-free medium. Wound images were observed at 0, 24, 48, and 72 h under an inverted microscope.

In vitro cell motility assay

The motility of cells was measured using transwell plates (Corning Costar, Cambridge, MA, USA) that were 6.5 mm in diameter with 8 μm pore filters. CNE2 cells which had been treated with rhHMGB1 or siHMGB1 in 200 μl of DMEM serum-free medium were seeded in upper chamber at a density of 5×10^5cells/well. The lower chambers were loaded with 600 μl of DMEM containing 20% FBS. After 24 h, the upper chambers were removed and fixed with 4% paraformaldehyde for 20 min. After staining with crystal violet solution, the filters were observed and photographed under an inverted microscope (Olympus).

In vitro cell invasion assay

A CNE2 cell suspension (200 μl, 5×10^5cells/ml) that had been treated with rhHMGB1 or siHMGB1 was added into the upper transwell chambers, which were pre-coated with matrigel (Corning, NY, USA), and 600 μl of DMEM with 20% FBS was added into the lower chamber. CNE2 cells were then incubated at 37°C for 24 h. The cells above the filters were carefully wiped out with a cotton swab, and the cells below the filters were stained by crystal violet solution, and then photographed under an inverted microscope (Olympus).

RNA interference

Human HMGB1 small interfering siRNA, negative control siRNA, human siRNA, and plasmids containing ALX/FPR2 or GPR32 were purchased from GenePharma, Inc. CNE2 cells were evenly plated in six-well plates with 10% FBS without antibiotics at the initial concentration of 5×10^4 cells/well. The cells were transfected with siRNA or siNC or plasmids using Lipofectamine 3000 reagent after reaching 60% confluency. Then, they were pre-treated with or without RvD1 (100 nM) for 2 h and cultured with or without rhHMGB1 (500 ng/ml). The groups transfected with HMGB1, ALX/FPR2 or GPR32 siRNA and control siRNA were labeled siHMGB1, siALX/FPR2, siGPR32, and siNC, respectively, and those transfected with plasmids were named OEALX/FPR2 and OEGPR32. The gene silencing and overexpression effects were detected by Western blot at 48 h post-transfection.

Statistical analyses

The data were presented as mean ± S.D. SPSS 17.0 software (IBM Corp, Armonk, NY, USA) was used for analysis. Statistical significance was assessed by unpaired Student's t-test and one-way analysis of variance. $P < 0.05$ denotes the presence of a statistically significant difference. Three replications were conducted in each assay.

Results

EMT markers, HMGB1 expression patterns in non-keratosis NPC and NPG tissues

To evaluate the expression of EMT markers in NPC, we performed immunohistochemistry (IHC) staining in 10 human NPC and 10 NPG tissue samples. The IHC staining of E-cadherin, vimentin, and HMGB1 in representative samples of NPC and NPG tissues is shown in Figure 1(a). NPC tissues lost their normal epithelial barrier and became disorganized. E-cadherin showed a decreasing trend in NPC, vimentin, and HMGB1 showed an unconspicuous increase. A semiquantitative evaluation of IHC staining was used to classify the expression of E-cadherin, vimentin, and HMGB1 in the samples (Figure 1(b)). There was significantly different expression of E-cadherin ($P < 0.05$) and HMGB1 ($P < 0.01$) in NPC and NPG tissues. HMGB1 was mostly located in the nuclei (Figure 1(c), red arrow) in NPG tissues, while more HMGB1 were found in cytoplasm in NPC tissues (Figure 1(d), black arrow). To confirm the EMT occurs in NPC tissues, we evaluated the expression of ZO-1, N-cadherin, E-cadherin, vimentin, and HMGB1 using Western blotting (Figure 1(e)). The epithelial markers (ZO-1, E-cadherin) were higher in NPG compared with NPC, while the mesenchymal markers (N-cadherin, vimentin) were lower in NPG compared with NPC. Expression of ZO-1, N-cadherin, E-cadherin, vimentin, and HMGB1 was significantly different ($P < 0.05$) (Figure 1(f)). Unlike these semiquantitative evaluations of IHC staining ($P > 0.05$), quantitative analyses of the expression of vimentin in the Western blot indicated a significant difference ($P < 0.05$). As protein quantification is more accurate than IHC

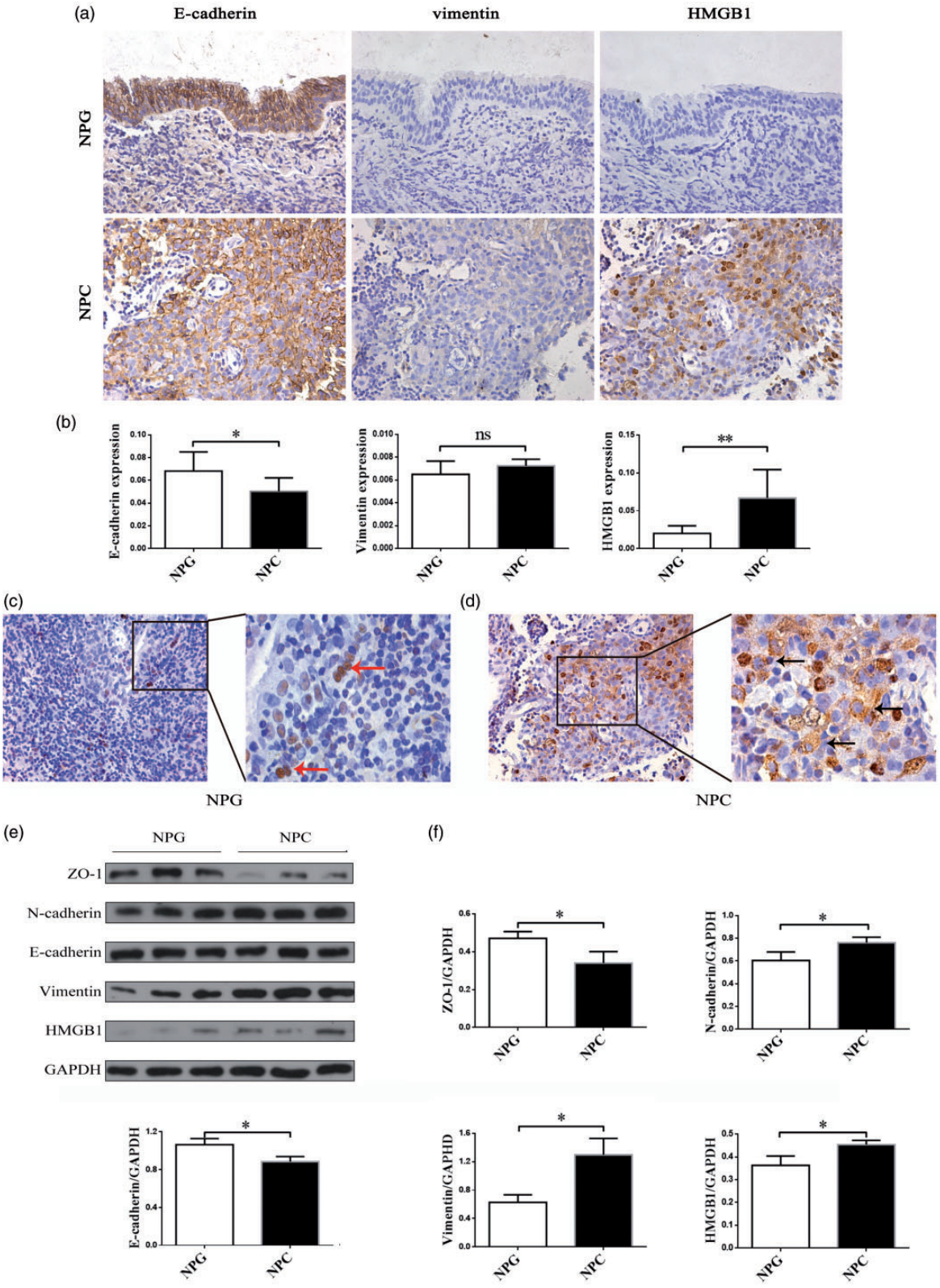

Figure 1. Expression of EMT markers and HMGB1 in non-keratosis NPC and NPG tissues. (a) An immunohistochemistry assay was performed to detect the staining of E-cadherin, vimentin, and HMGB1 in non-keratosis NPC and NPG tissues (×400). (b) The expression of E-cadherin, vimentin and HMGB1 in non-keratosis NPC and NPG tissues was determined by immunohistochemical semiquantification. Data are presented as mean ± SD. *$P < 0.05$, **$P < 0.01$. (NPC, n = 10 NPG, n = 10). (c, d) The location of HMGB1 in non-keratosis NPC and NPG tissues (×400, ×1000). The arrows show the location of HMGB1. (e) Protein expressions of ZO-1, N-cadherin, E-cadherin, vimentin, and HMGB1 were examined by Western blot. The experiment was performed in triplicate. (f) Quantitative analyses of EMT markers and HMGB1. Data are expressed as mean ± SD. *$P < 0.05$. The data represent the average of three experiments. (A color version of this figure is available in the online journal.) NPC: nasopharyngeal carcinoma; NPG: nasopharyngitis; GAPDH: glyceraldehyde 3-phosphate dehydrogenase; HMGB1: high mobility group box 1.

semiquantification, this suggests that the expression of vimentin was actually higher in the NPC tissues.

RhHMGB1 promoted EMT in CNE1 and CNE2 cell lines

EMT has been considered to induce metastasis of cancer cells. Western blot analysis showed that rhHMGB1 can significantly decrease the epithelial makers E-cadherin and ZO-1 and increase the mesenchymal markers N-cadherin and vimentin in both CNE1 (Figure 2(a)) and CNE2 (Figure 2(c)) cells. The results suggest that NPC cells transformed to an EMT phenotype after treatment with rhHMGB1 and the effect was dose dependent. The expression of vimentin in the CNE1 cells was not significantly different among the groups ($P > 0.05$), and the induction effect of rhHMGB1 was more obvious in CNE2 cells (Figure 2(b) and (d)).

The effect of siHMGB1 and rhHMGB1 on cell morphology, migration, and invasion

RhHMGB1-treated CNE2 cells showed a mesenchymal morphology transition and the cells had projecting pseudopodia (Figure 3(a)). A scratch assay was used to investigate migration of CNE2 cells at 24, 48, and 72 h (Figure 3(b)). The healing rate of CNE2 cells increased in the rhHMGB1-treated group compared with the control group and the siHMGB1 group (Figure 3(d)). To further confirm the effect of HMGB1 in the CNE2 cell invasion, we performed transwell migration and invasion assays (Figure 3(c)). The migration and invasion ability of rhHMGB1-incubated CNE2 cells dramatically increased ($P < 0.001$), while siRNA-mediated inhibition of HMGB1 induced the migration and invasion ability of CNE2 cells (Figure 3(e)). The migration and wound-healing assays revealed that cells transfected with siHMGB1 migrated more slowly than the rhHMGB1-treated and control cells. The invasion assay indicated that rhHMGB1 promoted NPC cell invasion ($P < 0.001$).

The effect of RvD1, rhHMGB1, and siHMGB1 on the expression of EMT markers in CNE2 cell lines

To further examine the relationship of HMGB1 with EMT in NPC and its possible inhibitors, we analyzed the

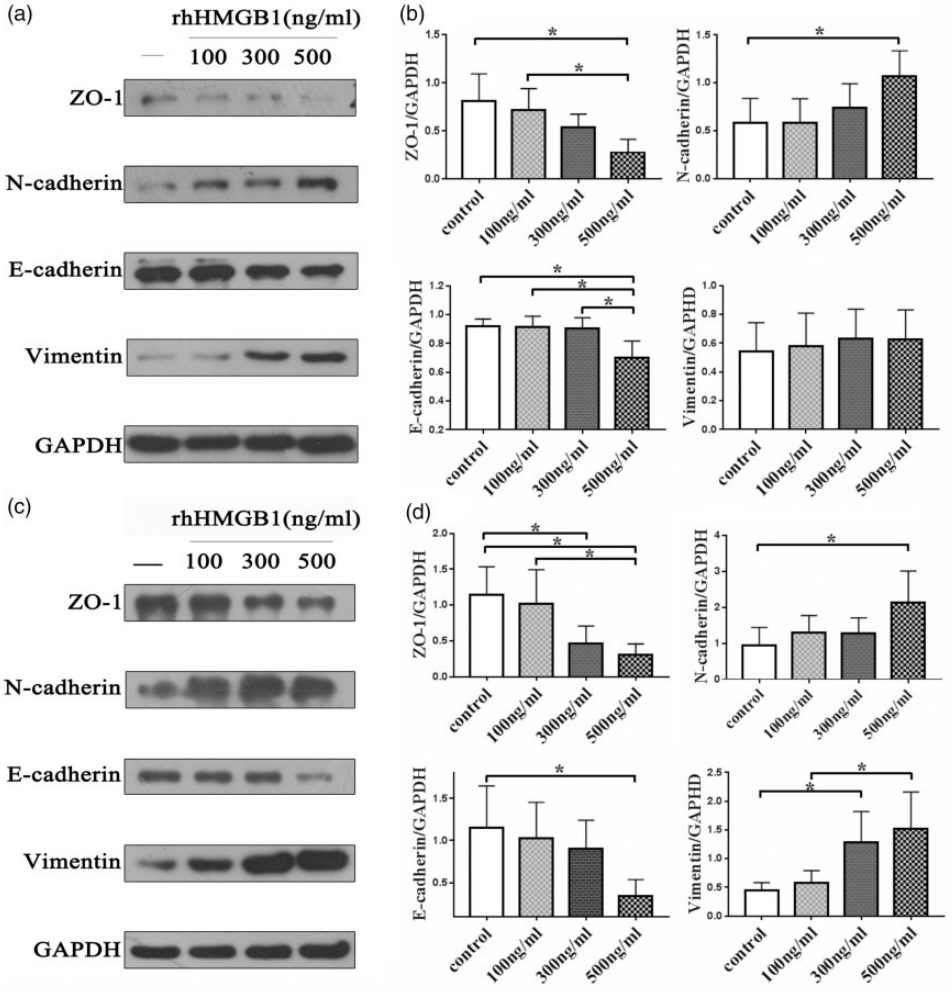

Figure 2. Expression of EMT markers in NPC cells (a) (c) Western blot assay was performed to detect the expression of ZO-1, N-cadherin, E-cadherin, vimentin, and GAPDH in CNE1 and CNE2 cells after treatment with dose-dependent rhHMGB1. Each experiment was performed in triplicate. (b) (d) Quantitative analyses of expression of EMT markers in CNE1 and CNE2 cells. Data are expressed as mean ± SD, *$P < 0.05$. The data represent the average of three experiments. rhHMGB1: recombinant human high mobility group box 1; GAPDH: glyceraldehyde 3-phosphate dehydrogenase.

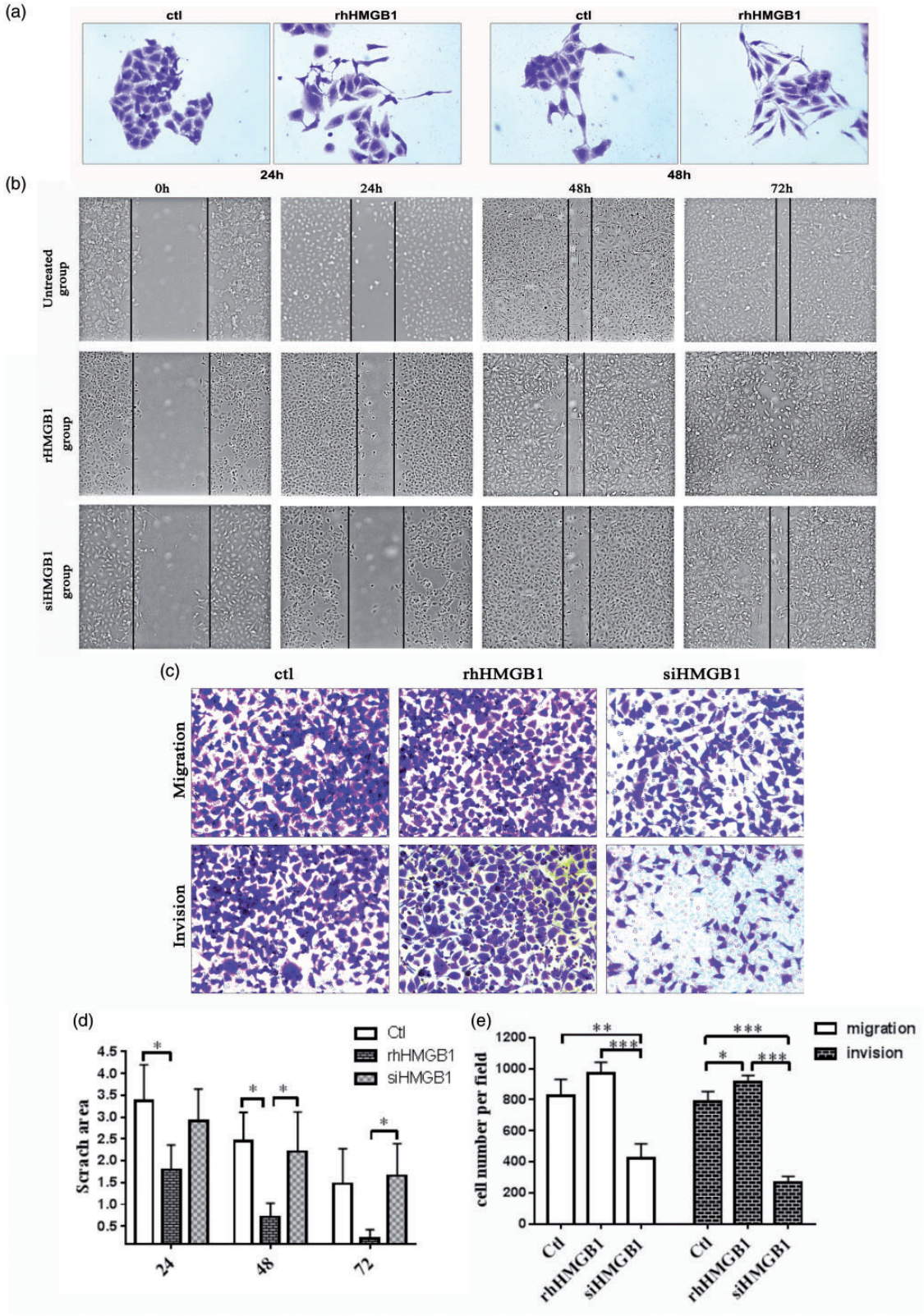

Figure 3. Effect of rhHMGB1 and siHMGB1 on CNE2 cell migration and invasion. (a) Microscopic (×100) images of CNE2 cells cultured with or without rhHMGB1 (500 ng/ml) for 24 h and 48 h. The experiment was performed in triplicate. (b) Images of scratch wound-healing assay captured under a microscope (×100) at 0 h, 24 h, 48 h, and 72 h. The experiment was performed in triplicate. (c) In transwell assays, knockdown of HMGB1 suppressed the migration and invasion ability of CNE2 cells compared with rhHMGB1 and control groups. The experiment was performed in triplicate. (d) Quantitative analyses of scratch area per group by time-point, $^{*}P < 0.05$. (e) Comparisons of cell number per field use migration and invasion assay of three groups of cells. $^{*}P < 0.05$, $^{**}P < 0.01$, $^{***}P < 0.001$. The data represent the average of three experiments. (A color version of this figure is available in the online journal.)

expression of ZO-1 and vimentin in different treated cells with confocal microscopy. The expression of ZO-1 increased in siHMGB1 and RvD1-treated groups compared with the control and rhHMGB1 groups (Figure 4(a)), and the expression of vimentin decreased in the siHMGB1 and RvD1-treated groups compared to the control and rhHMGB1 groups (Figure 4(b)). RvD1 and siHMGB1 up-regulated the expression of ZO-1 and E-cadherin while down-regulated the expression of N-cadherin and vimentin compared with the control and rhHMGB1-treated groups (Figure 4(c)).

Interaction between HMGB1 and RvD1 and its receptors

In order to illustrate the direct relationship between HMGB1 and RvD1 with its receptors, we measured the protein expression of HMGB1 after incubation CNE2 cell lines with RvD1 (100 nM) and expression of ALX/FPR2 and GPR32 after incubation with RvD1 and rhHMGB1. We found that RvD1 inhibited the expression of HMGB1 in CNE2 cell lines (Figure 5(a)). Expression levels of HMGB1 were significantly different ($P < 0.05$) (Figure 5(b)). The change of ALX/FPR2 was not obvious, while the expression of GPR32 slightly increased after treatment with rhHMGB1. Both the receptors increased after incubated with RvD1 (Figure 5(c)).

RvD1 inhibits HMGB1-induced EMT via ALX/FPR2 and GPR32 receptors

RvD1 inhibited rhHMGB1-induced EMT in a dose-dependent fashion (Figure 6(a)). To illustrate the mechanism of the active effects of RvD1 on EMT, the influence of gene silencing and over-expression of the receptors of RvD1 on the marker proteins of EMT were tested in CNE2 cells with and without rhHMGB1 treatment. The effects were verified by Western blot (Figure 6(b)).

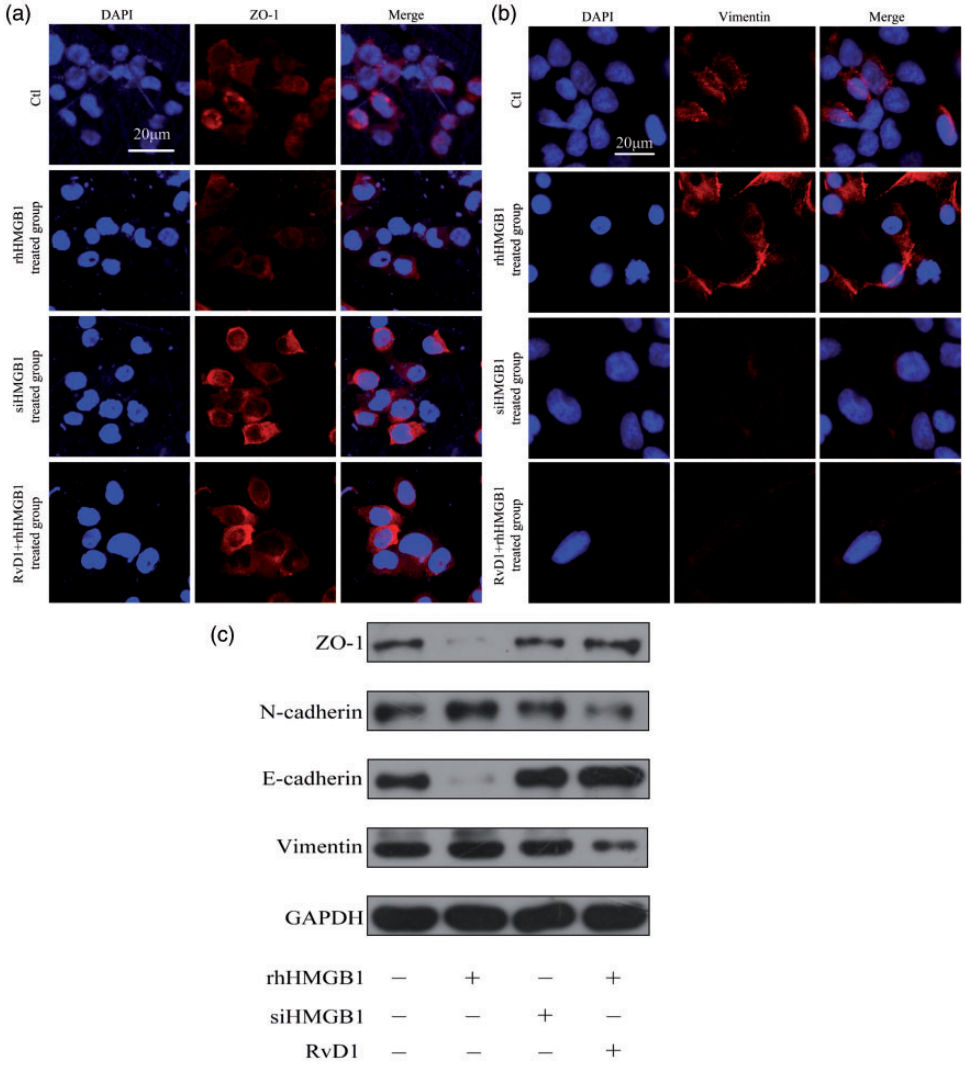

Figure 4. Confocal microscopic examination of ZO-1 and vimentin and protein expression of EMT markers in different groups of CNE2 cells. (a) Expression of ZO-1 in CNE2 cells. Scar bar, 20 μm. (b) Expression of vimentin in CNE2 cells. Scar bar, 20 μm. (c) Western blot assay was performed to detect the expression of ZO-1, N-cadherin, E-cadherin, vimentin, and GAPDH in CNE2 cells after treatment with rhHMGB1 (500 ng/ml), siHMGB1, or RvD1 (100 nM). Each experiment was performed in triplicate. (A color version of this figure is available in the online journal.)
GAPDH: glyceraldehyde 3-phosphate dehydrogenase.

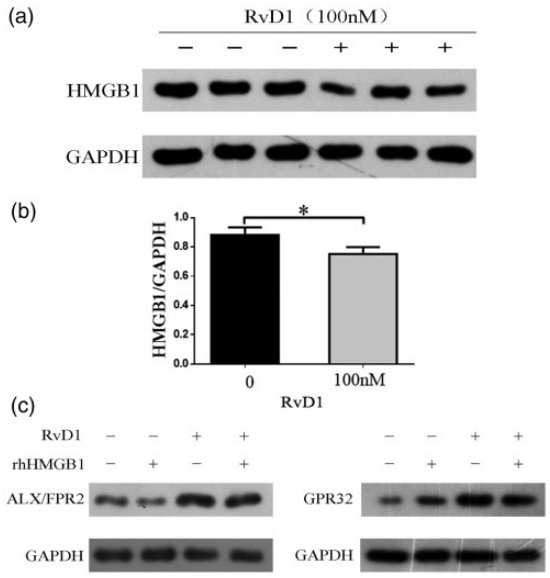

Figure 5. Interaction between HMGB1 and RvD1 and its receptors. (a) Western blot assay was performed to detect the expression of HMGB1 in CNE2 cells after treatment with RvD1 (100 nM). The experiment was performed in triplicate. (b) Quantitative analyses of expression of HMGB1 in CNE2 cells. Data are expressed as mean ± SD, *$P < 0.05$. The data represent the average of three experiments. (c) The expression of ALX/FPR2 and GPR32 after treatment with rhHMGB1 and RvD1. The experiment was performed in triplicate.
HMGB1: high mobility group box 1; RvD1: resolvin D1; FPR2: formyl peptide receptor 2; ALX: lipoxin A4 receptor; GAPDH: glyceraldehyde 3-phosphate dehydrogenase.

Increased expression of mesenchymal markers (N-cadherin and vimentin) induced by rhHMGB1 was attenuated by RvD1, and gene silencing of ALX/FPR2 or GPR32 reversed the effect. Reduced expression of ZO-1 and E-cadherin in rhHMGB1-treated CNE2 cells was restored by RvD1, while the silencing of receptor ALX/FPR2 or GPR32 eliminated the effects of RvD1. The inhibiting effect of RvD1 on HMGB1-induced EMT was enhanced by the overexpression of ALX/FPR2 or GPR32. This resulted in the recovery of ZO-1 and E-cadherin and reduction of N-cadherin and vimentin (Figure 6(c) and (d)). The results showed that RvD1 suppressed rhHMGB1-induced EMT via ALX/FPR2 and GPR32 receptors.

Discussion

Invasion and metastasis are characteristics of cancer cells and are related to the degree of malignancy and survival rate.[21] They are the main causes of death in patients with NPC, and some patients even have tumor metastasis at an early stage of the disease. An important contributor to cancer metastasis and invasion is EMT,[22] a cellular transition between epithelial and mesenchymal states. EMT has been reported in NPC in previous studies and is supported by our finding that the mesenchymal markers N-cadherin and vimentin were raised and epithelial markers,[23,24] ZO-1 and E-cadherin were decreased in NPC tissues compared with NPG tissues (Figure 1(a) and (e)). Among many cytokines which initiate EMT, HMGB1 was attached by scholars gradually. In our study, HMGB1 was observed to have increased significantly and translocated to the cytoplasm in the NPC tissue samples (Figure 1(c)). As a key mediator of inflammation, HMGB1 provides an active environment for cancers. Previous research has shown that HMGB1 can promote cancer development by inducing EMT.[25,26]

As a non-histone nuclear protein, HMGB1 regulates gene expression and processor of DNA repair, division, inflammation, cell death, apoptosis, and EMT.[27] Initially, HMGB1, mainly extracellular HMGB1, was identified and further studied as an important pro-inflammatory agent. An inflammatory environment partly maintains microenvironment for tumor growth. Consistent with previous studies, we demonstrated that HMGB1 was up-regulated and released from the nucleus and EMT was also found in NPC. In addition to the inflammatory environment, Epstein-Barr virus (EBV) infection is also an important factor in the increase of HMGB1 in patients with nasopharyngeal carcinoma. Zhu *et al.* demonstrated that HMGB1 can be induced by EBV infection, which is considered to be an important pathogen in NPC, and promotes the proliferation of human NPC cells.[28,29] Therefore, the elevation of HMGB1 may be related to EBV infection and inflammatory environment in NPC. We hypothesized the increased and translocated HMGB1 aggravate the occurrence of EMT in NPC. In our research, we found that rhHMGB1 treatment changed the expression of epithelial and mesenchymal markers. The expression of mesenchymal markers (N-cadherin and vimentin) was increased and epithelial markers (E-cadherin and ZO-1) were decreased (Figure 2). By transwell assay, rhHMGB1 enhanced invasion and migration of NPC cells (Figure 3). Furthermore, disrupting the expression of HMGB1 partly reversed the EMT induced by HMGB1. Gene silencing of HMGB1 inhibited the migration and invasion of NPC cell lines. This confirmed our hypothesis that increased and translocated HMGB1 indeed caused progress of NPC by promoting EMT (Figure 4). The molecular mechanism of HMGB1 causing EMT has been mentioned in previous studies.

Numerous studies had demonstrated that HMGB1 was an effective target to modulated EMT process in various cells. Inhibition of HMGB1 expression can result in the repression of EMT. Our findings are consistent with those previous studies. HMGB1 can bind to its receptor, i.e. RAGE to activate signaling pathways. Downstream signal pathway associated with RAGE involved in EMT including Cdc42/Rac, MAPK/NF-κB, and PI3K/AKT pathways. Silencing of HMGB1 in NPC cell lines may release EMT via reducing RAGE downstream signals.[27,30]

RvD1, an endogenous lipid mediator, has potent anti-inflammatory and pro-resolution actions in inflammation mediated by its receptors, GPR32, and ALX/FPR2. Its protective effect on inflammation has been reported in many diseases.[31–35] Its inhibiting effect on cancers has also been proposed.[36] In these studies, one vital anti-inflammatory mechanism of RvD1 is suppressing the inflammatory cytokines release including HMGB1.[37,38] In order to investigate the effect of RvD1 on HMGB1 in NPC cell lines, we assessed the expression of HMGB1 after incubation with RvD1 in CNE2 cell lines. The results showed that RvD1 suppressed the expression of HMGB1 (Figure 5(a)).

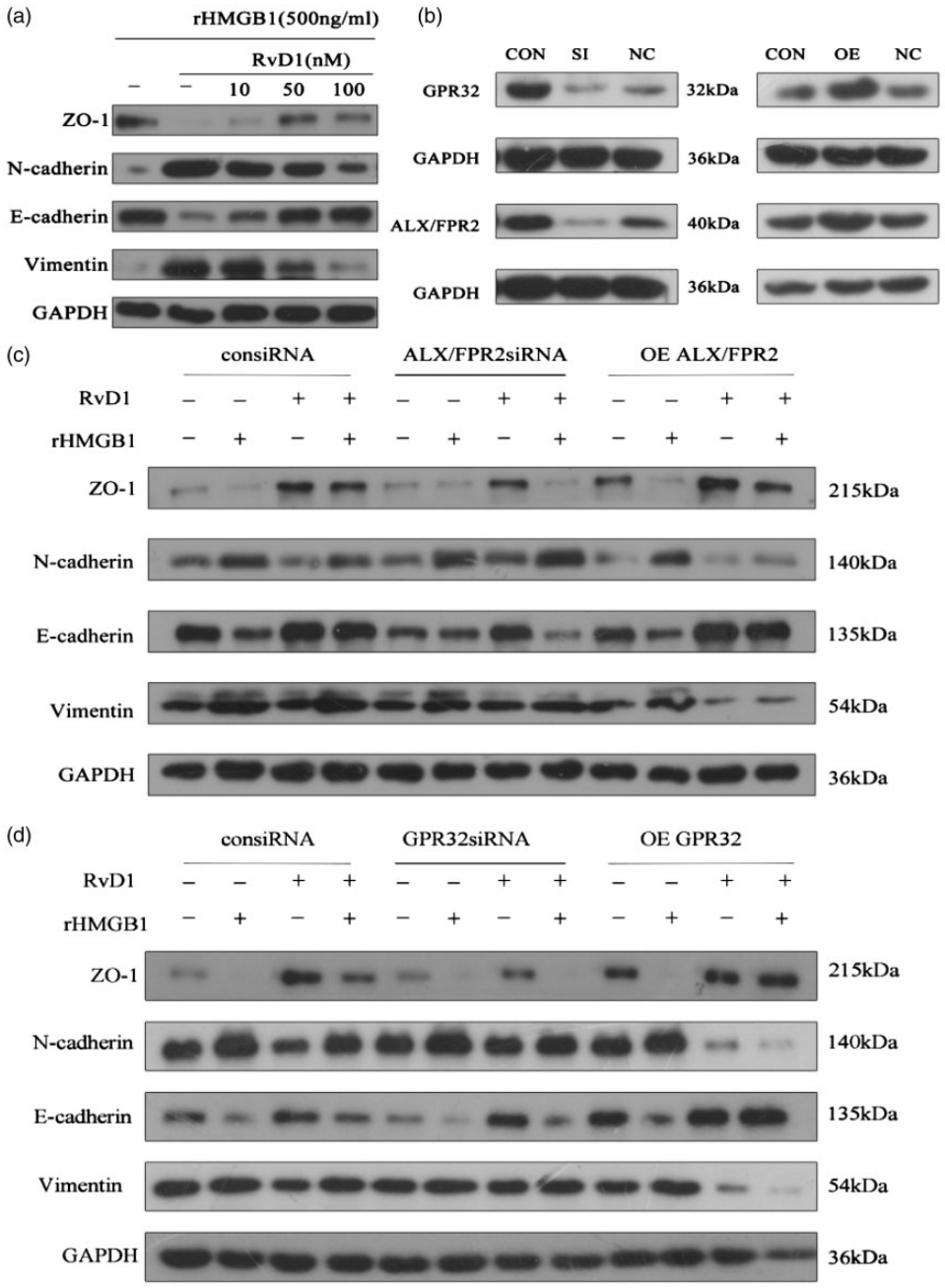

Figure 6. RvD1 suppression of rhHMGB1-induced EMT via ALX/FPR2 and GRP32 receptors in CNE2 cells. (a) RvD1 inhibited rhHMGB1-induced EMT and showed dose-dependent effects. (b) Effects of siRNA of ALX/FPR2 and GPR32 and plasmids containing ALX/FPR2 and GPR32 cDNA on CNE2 cells. (c) Effects of ALX/FPR2 gene silencing or over-expression on the change in EMT markers by RvD1 in rhHMGB1-induced EMT marker expression in CNE2 cells. Cells were transfected with siRNA of ALX/FPR2 or plasmid containing FPR2/ALX for 48 h. The cells were then cultured with or without rhHMGB1 (500 ng/ml) and RvD1 (100 nM). (d) Effects of GPR32 gene silencing or over-expression on the changes of EMT markers by RvD1 in rhHMGB1-induced EMT marker expression in CNE2 cells. Cells were transfected with siRNA of GPR32 or plasmid-containing GPR32 for 48 h. The cells were then cultured with or without rhHMGB1 (500 ng/ml) and RvD1 (100 nM). After incubation, the expressions of EMT markers were determined by Western blot. Each experiment was performed in triplicate.
Con: control; SI: siRNA; OE: overexpression; NC: control siRNA

Interestingly, HMGB1 and RvD1 influenced each other. HMGB1 as an important pro-inflammatory cytokine has been proven to suppress the capacity of phagocytosis partially through inducing the expression of 15-PGDH, which is an RvD1 inactivating enzyme. It suggested that HMGB1 has negative impact on the level of RvD1.[39] Meanwhile, RvD1 also can prevent the inflammasome assembly during inflammation, which is an important pathological process involved in the release of HMGB1.[40] In our study, we measured the protein expression of ALX/FPR2 and GPR32 after incubated with RvD1 and rhHMGB1. The results showed that the changes of ALX/FPR2 were not obvious after incubation with rhHMGB1, while the expression of GPR32 increased after treatment with RvD1 and rhHMGB1. RvD1 up-regulated the expression of the two receptors (Figure 5(c)).

In order to study the subsequent effect of RvD1 suppressed HMGB1, we evaluated the expression of EMT markers in CNE2 cell lines. We found that RvD1 significantly inhibited the expression of N-cadherin and vimentin and increased the expression of E-cadherin and ZO-1 in CNE2 cell lines. This subsequent effect is via the receptors GPR32 and ALX/FPR2, particularly GPR32. Overexpression of ALX/FPR2 and GPR32 and incubated with RvD1 significantly suppressed rhHMGB1-induced EMT, especially the expression of E-cadherin (Figure 6). RvD1 also can inhibit the expression of HMGB1-induced activation of NF-κB. NF-κB, which is an important transcription factor that regulated the expression of adhesion molecules and the expression of pro-inflammatory cytokines, can be inhibited by RvD1 and its activation is associated with increased HMGB1 acetylation and pronounced localization of HMGB1 in the cytoplasm.[41]

In our study, we found that RvD1 reversed the rhHMGB1-induced EMT and silenced the receptors of RvD1, GPR32 and ALX/FPR2, and reversed this protection effect in CNE2 cell lines. We postulate that RvD1 protects NPC cell lines via inhibiting the HMGB1/PI3K/AKT/GSK3β/β-catenin and MAPK/NF-κB pathway to improve the environment of cancers.

The other possible mechanism for the protective effect on RvD1 in NPC cell lines may be the membranous molecule RAGE, which functions as a receptor for HMGB1. Slowik *et al.* reported physiological interactions between RAGE and formyl peptide receptors (FPRs).[42] They found that RAGE ligands increased the expression of FPRs by altering the phosphorylation of ERK1/2. In our study, when rhHMGB1 stimulation was combined with overexpression of FPR2, EMT was strengthened, while the addition of RvD1 reversed this phenomenon. It may competitively bind to the receptor FPR2. The results support the hypothesis that RvD1 suppresses EMT in NPC via inhibiting HMGB1, partly by improving the inflammatory environment, and partly by competitive binding to receptor FPR2.

In summary, our results indicate that RvD1 suppressed rhHMGB1-induced EMT, and the protective effect was achieved by binding to the receptor FPR2 and GPR32. RvD1 may be a potential therapeutic strategy for NPC.

Authors' contributions: WK, YW, and PY were responsible for the experimental design. PY, SC, and GZ carried out the experiments; YW analyzed the data; PY and YW wrote the article. WK and YW supervised the project.

ACKNOWLEDGMENTS

The Institute of Otorhinolaryngology of Union Hospital supplied the necessary equipment and reagents.

DECLARATION OF CONFLICTING INTERESTS

The author(s) declared no potential conflicts of interest with respect to the research, authorship, and/or publication of this article.

FUNDING

This paper was supported by Wu Jieping Medical Foundation (No. LC1345) and the National Natural Science Foundation of China (No. 81873700).

ORCID iD

Pingli Yang https://orcid.org/0000-0002-5327-6751

REFERENCES

1. Ferlay J, Soerjomataram I, Dikshit R, Eser S, Mathers C, Rebelo M, Parkin DM, Forman D, Bray F. Cancer incidence and mortality worldwide: sources, methods and major patterns in GLOBOCAN 2012. *Int J Cancer* 2015;**136**:E359–E386
2. Wei WI, Sham JS. Nasopharyngeal carcinoma. *Lancet* 2005;**365**:2041–54
3. Lamouille S, Xu J, Derynck R. Molecular mechanisms of epithelial–mesenchymal transition. *Nat Rev Mol Cell Biol* 2014;**15**:178–96
4. Könnecke M, Burmeister M, Pries R, Böscke R, Bruchhage K, Ungefroren H, Klimek L, Wollenberg B. Epithelial–mesenchymal transition in chronic rhinosinusitis: differences revealed between epithelial cells from nasal polyps and inferior turbinates. *Arch Immunol Ther Exp* 2017;**65**:157–73
5. Lou Y, Diao L, Cuentas ERP, Denning WL, Chen L, Fan YH, Byers LA, Wang J, Papadimitrakopoulou VA, Behrens C, Rodriguez JC, Hwu P, Wistuba II, Heymach JV, Gibbons DL. Epithelial-Mesenchymal transition is associated with a distinct tumor microenvironment including elevation of inflammatory signals and multiple immune checkpoints in lung adenocarcinoma. *Clin Cancer Res* 2016;**22**:3630–42
6. Feng J, Cen J, Li J, Zhao R, Zhu C, Wang Z, Xie J, Tang W. Histone deacetylase inhibitor valproic acid (VPA) promotes the epithelial mesenchymal transition of colorectal cancer cells via up regulation of snail. *Cell Adh Migr* 2015;**9**:495–501
7. Liu CY, Xu JY, Shi XY, Huang W, Ruan TY, Xie P, Ding JL. M2-polarized tumor-associated macrophages promoted epithelial-mesenchymal transition in pancreatic cancer cells, partially through TLR4/IL-10 signaling pathway. *Lab Invest* 2013;**93**:844–54
8. Tong Z, Cai M, Wang X, Kong L, Mai S, Liu Y, Zhang H, Liao Y, Zheng F, Zhu W, Liu T, Bian X, Guan X, Lin MC, Zeng M, Zeng Y, Kung H, Xie D. EZH2 supports nasopharyngeal carcinoma cell aggressiveness by forming a co-repressor complex with HDAC1/HDAC2 and snail to inhibit E-cadherin. *Oncogene* 2012;**31**:583–94
9. Bianchi ME, Crippa MP, Manfredi AA, Mezzapelle R, Rovere QP, Venereau E. High-mobility group box 1 protein orchestrates responses to tissue damage via inflammation, innate and adaptive immunity, and tissue repair. *Immunol Rev* 2017;**280**:74–82
10. Amornsupak K, Jamjuntra P, Warnnissorn M, O-Charoenrat P, Sa-Nguanraksa D, Thuwajit P, Eccles SA, Thuwajit C. High ASMA(+) fibroblasts and low cytoplasmic HMGB1(+) breast cancer cells predict poor prognosis. *Clin Breast Cancer* 2017;**17**:441–52
11. Hu W, Liu PY, Yang YC, Chen PC, Su CM, Chao CC, Tang CH. Association of HMGB1 gene polymorphisms with lung cancer susceptibility and clinical aspects. *Int J Med Sci* 2017;**14**:1197–202
12. Chen X, Liu X, He B, Pan Y, Sun H, Xu T, Hu X, Wang S. MiR-216b functions as a tumor suppressor by targeting HMGB1-mediated JAK2/STAT3 signaling way in colorectal cancer. *Am J Cancer Res* 2017;**7**:2051–69
13. Pang X, Zhang Y, Zhang S. High-mobility group box 1 is overexpressed in cervical carcinoma and promotes cell invasion and migration in vitro. *Oncol Rep* 2017;**37**:831–40
14. Kang R, Xie Y, Zhang Q, Hou W, Jiang Q, Zhu S, Liu J, Zeng D, Wang H, Bartlett DL, Billiar TR, Zeh HR, Lotze MT, Tang D. Intracellular HMGB1 as a novel tumor suppressor of pancreatic cancer. *Cell Res* 2017;**27**:916–32
15. Hua S, Xiao L, Wu D. Effect of HMGB1 on proliferation of human nasopharyngeal carcinoma cell line C666-1 in vitro. *Nan Fang Yi Ke Da Xue Xue Bao* 2015;**35**:1540–5

16. Wu D, Ding Y, Wang S, Zhang Q, Liu L. *Increased expression of high mobility group box 1 (HMGB1) is associated with progression and poor prognosis in human nasopharyngeal carcinoma,* 2008;**216**:167–75
17. Recchiuti A. Resolvin D1 and its GPCRs in resolution circuits of inflammation. *Prostaglandins Other Lipid Mediat* 2013;**107**:64–76
18. Sok M, Tria MC, Olingy CE, San EC, Botchwey EA. Aspirin-triggered resolvin D1-modified materials promote the accumulation of pro-regenerative immune cell subsets and enhance vascular remodeling. *Acta Biomater* 2017;**53**:109–22
19. Zhang X, Wang T, Gui P, Yao C, Sun W, Wang L, Wang H, Xie W, Yao S, Lin Y, Wu Q. Resolvin D1 reverts lipopolysaccharide-induced TJ proteins disruption and the increase of cellular permeability by regulating IκBα signaling in human vascular endothelial cells. *Oxid Med Cell Longev* 2013;**2013**:185715
20. Lee HJ, Park MK, Lee EJ, Lee CH. Resolvin D1 inhibits TGF-β1-induced epithelial mesenchymal transition of A549 lung cancer cells via lipoxin A4 receptor/formyl peptide receptor 2 and GPR32. *Int J Biochem Cell Biol* 2013;**45**:2801–7
21. Steeg PS. Tumor metastasis: mechanistic insights and clinical challenges. *Nat Med* 2006;**12**:895–904
22. Nieto MA, Huang RY, Jackson RA, Thiery JP. EMT: 2016. *Cell* 2016;**166**:21–45
23. Song LB, Li J, Liao WT, Feng Y, Yu CP, Hu LJ, Kong QL, Xu LH, Zhang X, Liu WL, Li MZ, Zhang L, Kang TB, Fu LW, Huang WL, Xia YF, Tsao SW, Li M, Band V, Band H, Shi QH, Zeng YX, Zeng MS. The polycomb group protein bmi-1 represses the tumor suppressor PTEN and induces epithelial-mesenchymal transition in human nasopharyngeal epithelial cells. *J Clin Invest* 2009;**119**:3626–36
24. Horikawa T, Yang J, Kondo S, Yoshizaki T, Joab I, Furukawa M, Pagano JS. Twist and epithelial-mesenchymal transition are induced by the EBV oncoprotein latent membrane protein 1 and are associated with metastatic nasopharyngeal carcinoma. *Cancer Res* 2007;**67**:1970–8
25. Liu PL, Liu WL, Chang JM, Chen YH, Liu YP, Kuo HF, Hsieh CC, Ding YS, Chen WW, Chong IW. MicroRNA-200c inhibits epithelial-mesenchymal transition, invasion, and migration of lung cancer by targeting HMGB1. *Plos One* 2017;**12**:e180844
26. Musumeci D, Roviello GN, Montesarchio D. An overview on HMGB1 inhibitors as potential therapeutic agents in HMGB1-related pathologies. *Pharmacol Ther* 2014;**141**:347–57
27. Chen YC, Statt S, Wu R, Chang HT, Liao JW, Wang CN, Shyu WC, Lee CC. High mobility group box 1-induced epithelial mesenchymal transition in human airway epithelial cells. *Sci Rep* 2016;**6**:18815
28. Fae DA, Martorelli D, Mastorci K, Muraro E, Dal Col J, Franchin G, Barzan L, Comaro E, Vaccher E, Rosato A, Dolcetti R. *Broadening Specicity and Enhancing Cytotoxicity of Adoptive T Cells for Nasopharyngeal Carcinoma Immunotherapy,* 2016;**4**:431–440
29. Zhu X, Sun L, Wang Y. High mobility group box 1 (HMGB1) is upregulated by the Epstein-Barr virus infection and promotes the proliferation of human nasopharyngeal carcinoma cells. *Acta Oto-Laryngol* 2015;**136**:87–94
30. Buckley ST, Ehrhardt C. The receptor for advanced glycation end products (RAGE) and the lung. *J Biomed Biotechnol* 2010;**2010**:917108
31. Zhang SK, Zhuo YZ, Li CX, Yang L, Gao HW, Wang XM. Xuebijing injection () and resolvin D1 synergize regulate leukocyte adhesion and improve survival rate in mice with Sepsis-Induced lung injury. *Chin J Integr Med* 2018;**24**:272–7
32. Villar J, Cabrera-Benitez NE, Valladares F, Garcia-Hernandez S, Ramos-Nuez A, Martin-Barrasa JL, Muros M, Kacmarek RM, Slutsky AS. Tryptase is involved in the development of early ventilator-induced pulmonary fibrosis in sepsis-induced lung injury. *Crit Care* 2015;**19**:138
33. Grabiec AM, Hussell T. The role of airway macrophages in apoptotic cell clearance following acute and chronic lung inflammation. *Semin Immunopathol* 2016;**38**:409–23
34. Masterson C, Devaney J, Horie S, O'Flynn L, Deedigan L, Elliman S, Barry F, O'Brien T, O'Toole D, Laffey JG. Syndecan-2-positive, bone marrow-derived human mesenchymal stromal cells attenuate bacterial-induced acute lung injury and enhance resolution of ventilator-induced lung injury in rats. *Anesthesiology* 2018;**129**:502–16
35. Wang Q, Zheng X, Cheng Y, Zhang LY, Wen XH, Tao Z, Li H, Hao Y, Gao Y, Yang ML, Smith GF, Huang JC, Jin WS. Resolvin D1 stimulates alveolar fluid clearance through alveolar epithelial sodium channel, Na, K-ATPase via ALX/cAMP/PI3K pathway in lipopolysaccharide-induced acute lung injury. *J Immunol* 2014;3765–77
36. Zhong X, Lee HN, Surh YJ. RvD1 inhibits TNFalpha-induced c-Myc expression in normal intestinal epithelial cells and destabilizes hyper-expressed c-Myc in colon cancer cells. *Biochem Biophys Res Commun* 2018;**496**:316–23
37. Kang JW, Choi HS, Shin JK, Lee SM. Resolvin D1 activates the sphingosine-1-phosphate signaling pathway in murine livers with ischemia/reperfusion injury. *Biochem Biophys Res Commun* 2019;**514**:1058–65
38. Murakami T, Suzuki K, Tamura H, Nagaoka I. Suppressive action of resolvin D1 on the production and release of septic mediators in D-galactosamine-sensitized endotoxin shock mice. *Exp Ther Med* 2011;**2**:57–61
39. Kang GJ, Lee HJ, Kang YP, Kim EJ, Kim HJ, Byun HJ, Park MK, Cho H, Kwon SW, Lee CH. High-mobility group box 1 suppresses resolvin D1-induced phagocytosis via induction of resolvin D1-inactivating enzyme, 15-hydroxyprostaglandin dehydrogenase. *Biochim Biophys Acta* 2015;**1852**:1981–8
40. Mottola G, Chatterjee A, Wu B, Chen M, Conte MS. Aspirin-triggered resolvin D1 attenuates PDGF-induced vascular smooth muscle cell migration via the cyclic adenosine monophosphate/protein kinase A (cAMP/PKA) pathway. *Plos One* 2017;**12**:e174936
41. Wang M, Gorasiya S, Antoine DJ, Sitapara RA, Wu W, Sharma L, Yang H, Ashby CJ, Vasudevan D, Zur M, Thomas DD, Mantell LL. The compromise of macrophage functions by hyperoxia is attenuated by ethacrynic acid via inhibition of NF-kappaB-mediated release of high-mobility group box-1. *Am J Respir Cell Mol Biol* 2015;**52**:171–82
42. Slowik A, Merres J, Elfgen A, Jansen S, Mohr F, Wruck CJ, Pufe T, Brandenburg LO. Involvement of formyl peptide receptors in receptor for advanced glycation end products (RAGE)–and amyloid beta 1-42-induced signal transduction in glial cells. *MOL Neurodegener* 2012;**7**:55

(Received April 11, 2019, Accepted September 19, 2019)